Probing the ISM of a Starburst Galaxy at z = 3.8 with medium-resolution spectroscopy

Rémi CABANAC (LATT, Université de Toulouse, CNRS, France), Matthew HAYES, Daniel SCHAERER, Anne VERHAMME (Observatoire de Genève),
David VALLS-GABAUD (GEPI, CNRS, OPM, France), Christopher LIDMAN (ESO, Chile), Lise CHRISTENSEN (ESO, Chile)

ABSTRACT We recently reported the discovery of FORJ0332-3557, a lensed Lyman-break galaxy at z = 3.77 in a remarkable example of strong galaxy-galaxy gravitational lensing. We present here a medium-resolution rest-frame UV spectrum of the source, which appears to be similar to the well-known Lyman-break galaxy MS1512-cB58 at z = 2.73.
The spectral energy distribution is consistent with a stellar population of less than 30 Ma, with an extinction of A_V = 0.5 mag and an extinction-corrected star formation rate SFR_{UV} of 200-300 h_{70}^{-1} $M_\odot$ a^{-1}. The Lyman-α line exhibits a damped profile in absorption produced by a column density of about N_{HI} = (2.5 ± 1.0) x 10^{21} cm^{-2}, superimposed on an emission line shifted both spatially (0.5arcsec with respect to the UV continuum source) and in velocity space (+830 km s^{-1}) with respect to the low-ionisation absorption lines from its interstellar medium), a clear signature of outflows with an expansion velocity of about 270 km s^{-1}. A strong emission line from HeII λ164.04 nm indicates the presence of Wolf-Rayet stars and reinforces the interpretation of a very young starburst. The metallic lines indicate sub-solar abundances of elements Si, Al, and C in the ionised gas phase.

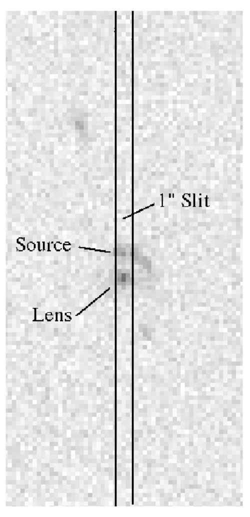

VLT/FORS2 acquisition frame (in the R band) and 1 arcsec-slit mask position on FORJ0332-3557: the central object is the lens at z~1 and the top arc is the lensed Lyman break galaxy at z~3.77.

Table 1. Description of spectroscopic data with *VLT/FORS2*.

Date UT time y-m-d h:m:s	exp. time s	airmass -	seeing ″	slit ″
2004-11-16 01:02:19	1495	1.446	0.56	1.0
2004-11-16 01:28:01	1495	1.326	0.55	1.0
2004-11-16 01:54:29	1495	1.231	0.65	1.0
2004-11-16 02:20:09	1495	1.161	0.76	1.0
2005-01-30 01:20:45	1495	1.103	0.50	1.0
2005-01-30 01:46:26	1495	1.154	0.54	1.0
2006-10-16 06:02:29	1400	1.028	0.66	0.8
2006-10-16 06:26:57	1400	1.020	0.53	0.8
2006-10-16 06:51:33	1400	1.021	0.61	0.8
2006-10-16 07:15:52	1400	1.031	0.50	0.8
2006-10-16 07:55:52	1400	1.068	0.73	0.8
2006-10-16 08:20:31	1400	1.104	0.61	0.8
2006-10-21 07:37:59	1400	1.070	0.48	0.8
2006-10-21 08:02:09	1400	1.106	0.61	0.8
2006-11-21 07:03:26	1400	1.266	0.85	0.8
2006-11-22 04:33:11	1400	1.023	0.85	0.8
2006-11-22 04:57:20	1400	1.036	0.89	0.8
2006-11-28 04:24:07	1400	1.030	0.54	0.8
2006-11-28 04:48:36	1400	1.048	0.63	0.8
2006-11-28 05:20:59	1400	1.087	0.50	0.8
2006-11-28 05:45:14	1400	1.130	0.57	0.8
2007-01-25 04:30:28	1400	1.916	0.67	0.8

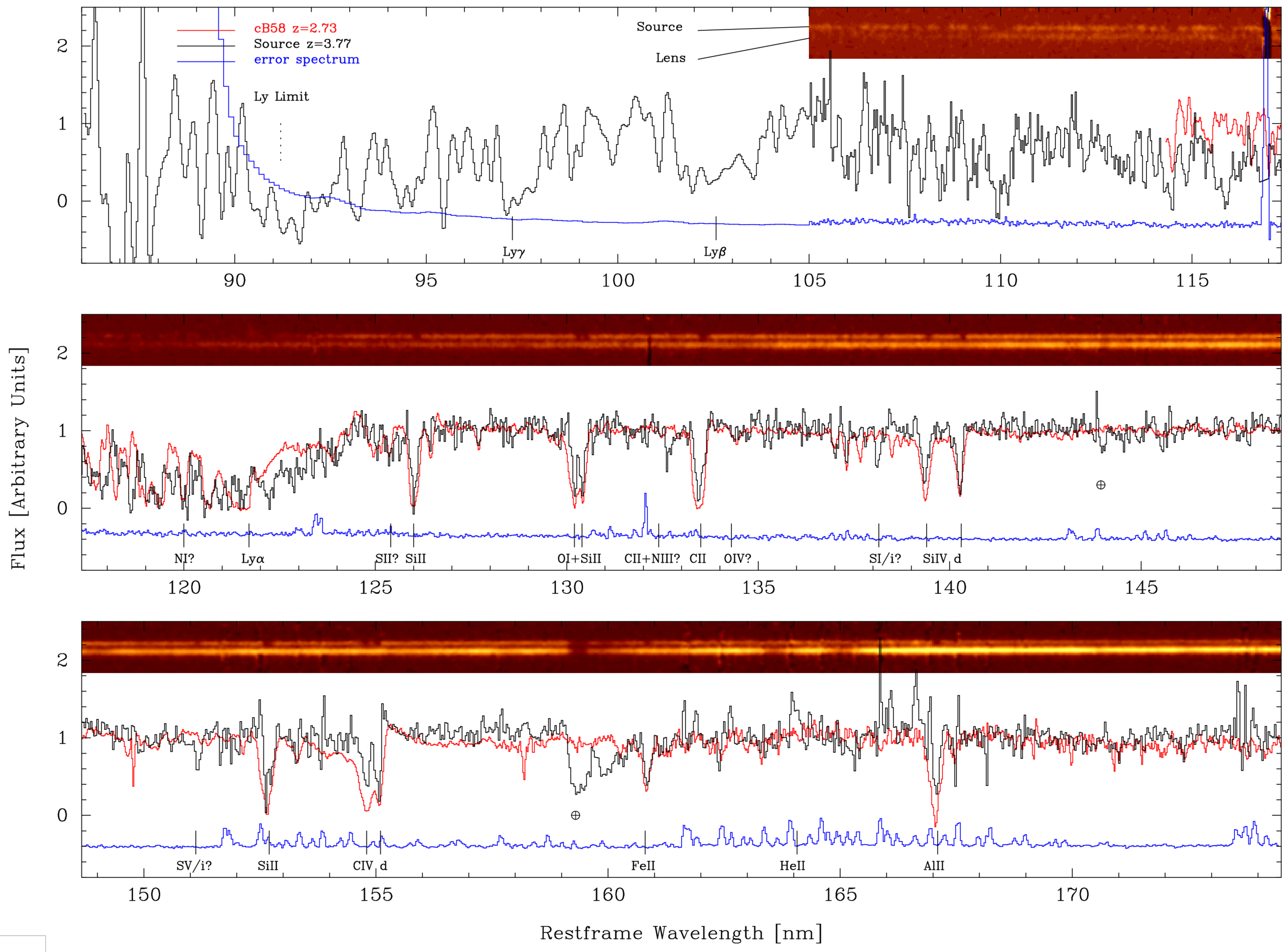

Table 2. Interstellar absorption lines

Ion	λ_{vac}^{lab} nm	λ_{vac}^{obs} nm	redshift	$W_0{}^a$ nm	f	$\log N^b$ cm^{-2}	$[X/H]_\odot{}^c$	Comments
H I Lyγ	97.254	-	-	$1.50 \pm 0.30^{+0.20}_{-0.10}$	0.0290	-	-	
H I Lyβ	102.57	-	-	$2.10 \pm 0.80^{+0.80}_{-0.60}$	0.07912	-	-	
H I Lyα	1215.7	-	-	-	0.4164	21.4 ± 0.2	-	
He II	164.04	783.09	3.7738	$-0.22 \pm 0.01^{+0.02}_{-0.02}$	-	-	-	WR feature
C II	133.45	637.01	*3.7732*	$0.21 \pm 0.03^{+0.03}_{-0.02}$	0.1278	15.019 ± 0.10	> -2.8	blended with C II*λ133.57
C IV	154.82	738.74	3.7716	$0.10 \pm 0.03^{+0.06}_{-0.03}$	0.1908	14.40 ± 0.21	> -3.6	
C IV	155.08	740.00	*3.7718*	$0.19 \pm 0.05^{+0.02}_{-0.02}$	0.09522	14.97 ± 0.25	> -3.0	sky contamination
N I?	~ 120	572.70	*3.7718*	$0.36 \pm 0.18^{+0.08}_{-0.05}$	0.04023	15.84 ± 0.25	$-1.6?$	triplet N Iλ 119.95 120.02 120.07
N III?	132.43	632.24	*3.7741*	-	-	-	-	blended with C IIλ132.39
O I	130.22	621.31	*3.7714*	$0.15 \pm 0.03^{+0.05}_{-0.03}$	0.04887	15.30 ± 0.17	> -3.0	blended with Si IIλ130.44
O IV	134.34	641.27	3.7735	$0.14 \pm 0.01^{+0.05}_{-0.03}$	-	-	-	photospheric
Al II	167.08	797.41	*3.7726*	$0.19 \pm 0.02^{+0.07}_{-0.03}$	1.833	13.62 ± 0.22	> -2.5	sky contamination
S I/i?	138.16	659.29	3.7719	$0.11 \pm 0.01^{+0.03}_{-0.02}$	-	-	-	
S II/i?	125.38	598.57	3.7740	$0.12 \pm 0.02^{+0.04}_{-0.05}$	0.01088	15.90 ± 0.15	$-1.1?$	
S II/i?	125.95	601.31	*3.7742*	$0.19 \pm 0.04^{+0.03}_{-0.02}$	0.01624	-	-	blended with Si II λ126.04
S V?	150.18	716.39	*3.7741*	$0.3 \pm 0.03^{+0.04}_{-0.2}$	0.00545	-	-	photospheric
S II/i?	151.12	721.43	*3.7740*	$0.07 \pm 0.01^{+0.02}_{-0.02}$	-	-	-	blended with Si IIλ151.21
Si II	126.04	601.84	*3.7749*	$0.19 \pm 0.04^{+0.03}_{-0.02}$	1.007	14.13 ± 0.11	> -2.8	blended with S IIλ125.95
Si II	130.47	622.49	*3.7710*	$0.16 \pm 0.01^{+0.06}_{-0.03}$	0.094	15.05 ± 0.37	$-1.9?$	blended with O Iλ130.22
Si II	152.67	728.39	3.7710	$0.24 \pm 0.03^{+0.02}_{-0.02}$	0.130	14.96 ± 0.11	> -2.0	
Si II*?	153.34	731.40	3.7697	$0.04 \pm 0.01^{+0.01}_{-0.01}$	0.132	14.20 ± 0.10	$-2.8?$	
Si IV	139.38	665.09	3.7718	$0.19 \pm 0.03^{+0.03}_{-0.02}$	0.5140	14.33 ± 0.10	> -2.6	
Si IV	140.28	669.38	*3.7718*	$0.21 \pm 0.03^{+0.04}_{-0.02}$	0.2553	14.66 ± 0.12	> -2.3	blended with S Iλ140.15?
Fe II	160.84	767.68	3.7728	$0.12 \pm 0.02^{+0.01}_{-0.02}$	0.058	14.95 ± 0.11	-2.0	

[a] Errors are given as statistical (±photon noise) and systematic ($^+_-$systematic uncertainty in location of the continuum)
[b] Lower limits based on the assumption of an optically thin medium
[c] Assuming solar abundances from Asplund et al. (2005)

The spectrum of FORJ0332-3557 shows characteristic absorption lines from starburst galaxies. They are summarised in Table~2. The medium-resolution spectrum of the LBG cB58 (Pettini 2000) is shown in Figure above in red, superimposed on our source, for a direct comparison of the insterstellar features. It is immediately obvious that the FORJ0332-3557 source is qualitatively similar to cB58.
All common interstellar absorptions are found in FORJ0332-3557. The strong absorption features include low-ionisation lines associated with neutral gas (SiII $\lambda\lambda\lambda$126.04 130.47 152.67, CII λ133.45, OI λ130.22, Al II λ167.08, FeII λ160.84) and high-ionisation lines associated with a hot gas phase (Si IV $\lambda\lambda$139.38 140.28, CIV $\lambda\lambda$154.82 155.08). Table 2 lists the ion line identification, vacuum rest-frame wavelength λ_{vac}^{lab}, observed wavelength λ_{vac}^{obs} , redshift z, rest-frame equivalent width W_0, oscillator strengths f, column density, ion abundance with respect to solar $[X/H]_\odot$ and comments. Additional uncertain identifications are question-marked, the lines noted *i?* might belong to interlopers at unknown redshift(s). We emphasize that the derived W_0 are very sensitive to both sky subtraction and continuum normalisation, hence the systematic errors caused by the continuum normalisation have tentatively been computed and are shown to be close to photon counting errors, while the sky subtraction error is much more difficult to quantify. As a sanity check, we computed the equivalent widths of absorption lines in the spectrum of cB58 and found our measurements to be fully consistent with those published by (Pettini 2002).
No nebular emission lines are detected in the present spectrum other than HeII λ164.04nm (*S~f{HeII}*). A weak detection of CIII] λ190.87 seen on a previous spectrum (Cabanac 2005) suggests that contamination of the high-ionisation lines by nebular emission is present but small. P-Cygni profiles are visible on CII λ133.45, and CIV λ155.08.
There are several ways to derive the abundances in the interstellar medium of distant galaxies (Spitzer 1978, Pettini 2002, Savaglio 2002). Ideally one should build a curve of growth by fitting Voigt profiles and Doppler parameters b for all ions independently. Because the resolution of our observed spectrum is just under the resolution one needs for Voigt profile fitting, and is penalised by a low signal-to-noise ratio, most of the strong lines appear saturated, and most weak lines are dominated by noise.
A careful analysis of the ISM metallicity goes beyond the present paper and will be done elsewhere. Here we present only qualitative arguments on the curve of growth, and Doppler parameters b. Assuming that the interstellar medium in FORJ0332-3557 is optically thin, one can infer lower limits to column densities, log(N[cm^{-2}]), and abundances (given in Table 2) by taking the optically thin approximation

$$\log N\ [cm^{-2}] = 19.053 + \log[\ W_\lambda / \lambda^2 f\ ]\ ,$$

where f is the line oscillator strength. The equivalent width, W_λ, and the wavelength λ are in nm. A tentative curve of growth indicates that the ion abundances could be 2-3 dex larger for a Doppler parameter of b = 50 km s^{-1}. In this context, the most constraining line, besides Si II* λ153.3 which may be blended, is FeII λ160.8, which appears unsaturated and whose small equivalent width is similar to the one measured in cB58 and would yield b ~ 60 km s^{-1}, similar to the b ~ 70 km s^{-1} reported in cB58 (Pettini 2002).
Compared to cB58, FORJ0332-3557 W_0 are lower by factors of 2-3 (CIV $\lambda\lambda$155.08 155.08, Al II λ167.08, OI λ130.22) to a factor of 1-1.2 (Si IV $\lambda\lambda$139.38 140.28, Fe II λ160.84).

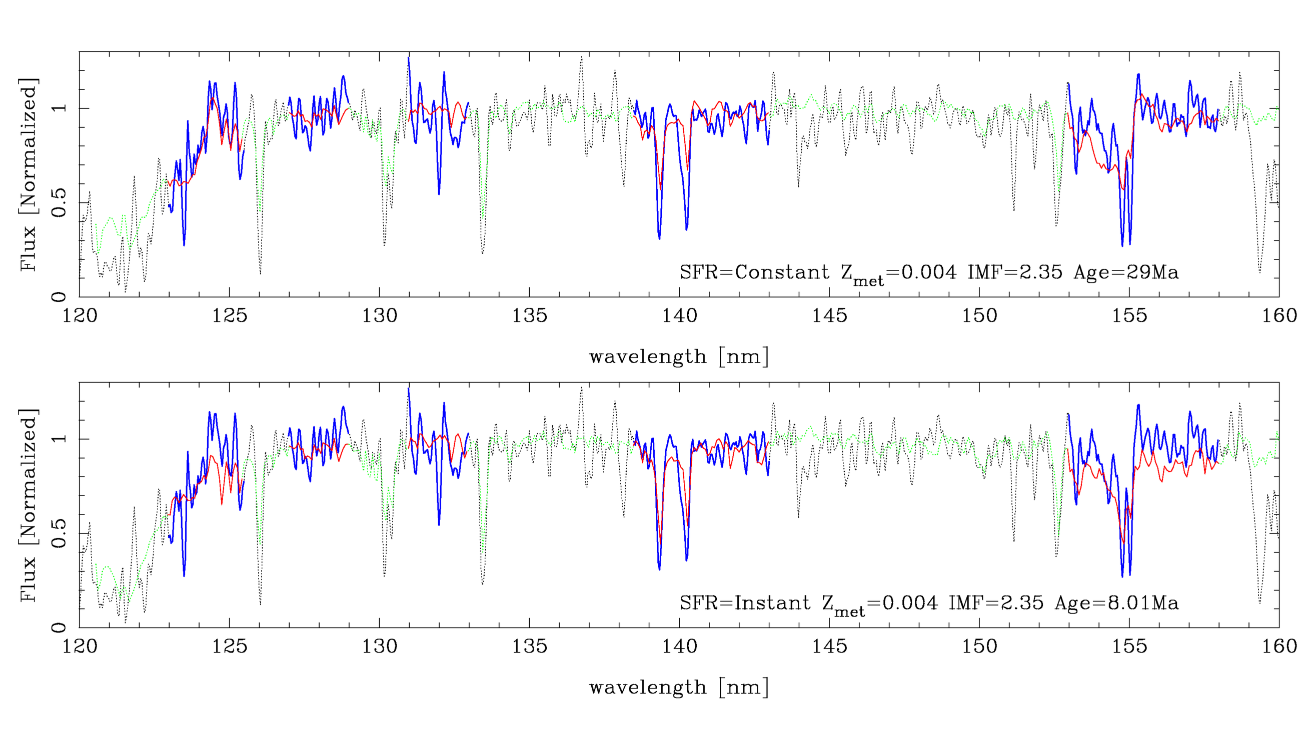

The best fit starburst99 models (red lines) are overlaid on the normalised spectrum of FORJ0332-3557 source (blue line) for two extreme scenarios of star formations with a Salpeter IMF from 1-100 $M_\odot$, at a metallicity Z_{metal}=0.004 (1/5 $Z_\odot$). The parts of the spectrum excluded of the fit are shown as dotted lines (see text). The top frame shows a constant SFR for 29 Ma. Ages older than 20 Ma are strongly favoured. The bottom frame shows an 8 Ma-old instantaneous burst of star formation. No model (at any available metallicities (1/20 $Z_\odot$) can reproduce the observed depths of the lines. For a constant SFR, larger metallicities produce older ages (29 Ma at Z_{metal} = 0.001, >49 Ma at Z_{metal} = 0.008). Instantaneous burst models tend to produce deeper lines while constant SFR models tend to better fit the observed P-Cygni profiles of CIV λ155.08 nm.

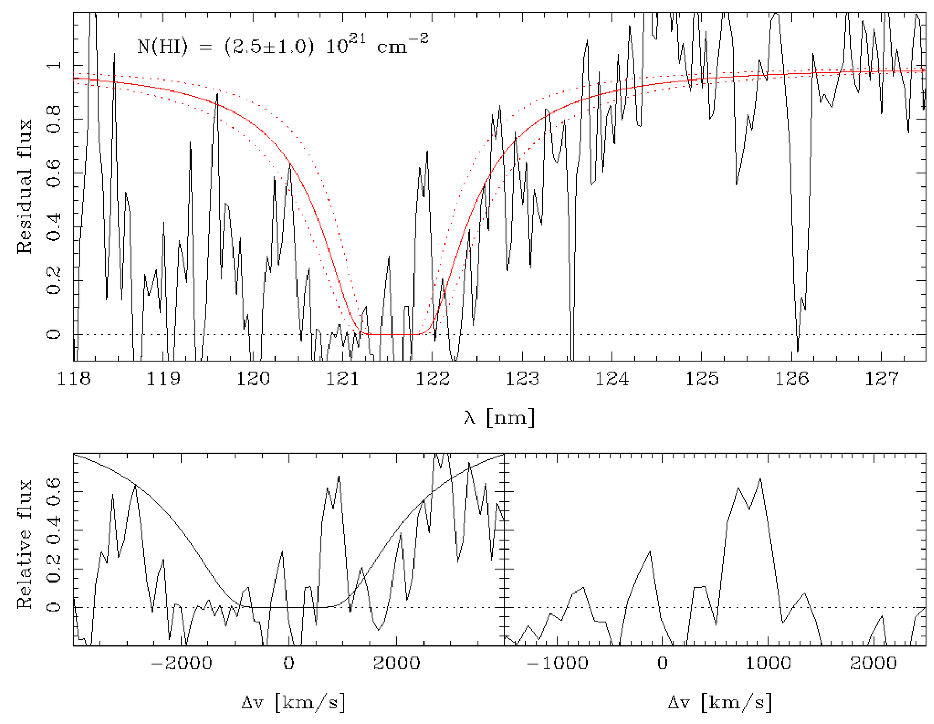

The best-fit Voigt profile corresponding to a column density of 2.5±1x$10^{21}$$cm^{-2}$(solid and red dotted lines) is shown on the rest-frame spectrum (top frame).The bottom frames show the same fit in velocity space Δv.
On the panel at the bottom right the model is subtracted out of the spectrum,showing a conspicuous emission feature peaking at ~830 km/s. This feature is also offset spatially by 2 pixels (ca. 0.5arcsec) from the main UV-continuum emitting source (see Fig. below)

The best-fit Ly-a profile of an expanding shell To fit the profile high N_H + dust is always needed.
- Typically log(N_H)>21.3 (at 1 sigma), but best fits are for 21.7. Again, this is higher than N_H obtained from Voigt profile fitting..

- The small "Lya peak" found at ~800-1000 km/s can be reproduced with shells of vexp~100 km/s, which is consistent with our velocity measured between the IS and 2 photospheric lines.
Higher vexp values are difficult to reconcile, since the peak is then expected at higher v.

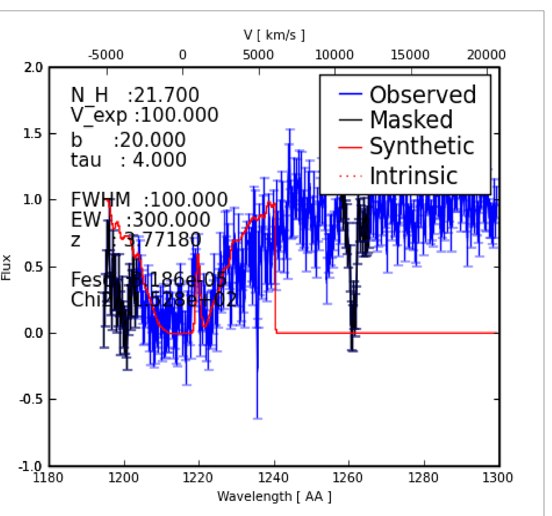

- EW>~100 Ang is required to get the Lya peak - again, as expected for SFR~const (and from cB58 modeling).

- Here the peak is found at higher velocity than the 1st-order value v_peak~2* v_exp given in Verhamme (2006). This is due to the very high N_H. This effect was also mentioned in Verhamme+08, where we explain the observed increase of the Lya-IS shift in LBGs when moving to strong absorption objects.

- Concerning the dust amount: one finds typically tau~1-4, which corresponds to E(B-V)~0.1-0.4 for a Calzetti law. Assuming E(B-V)=0.4, this would correspond to E(B-V)~0.26 for a SMC law.

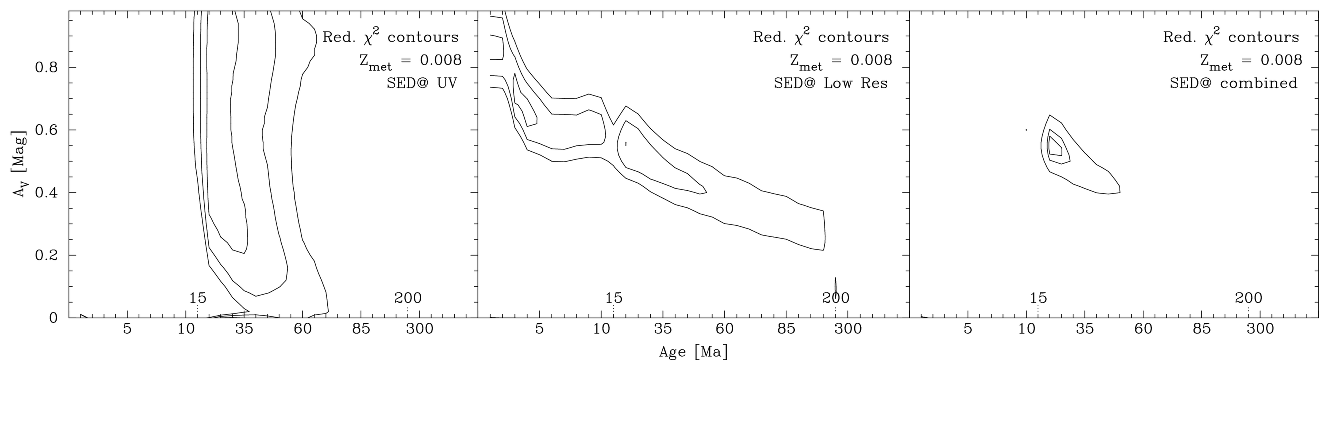

Reduced χ^2 contours are given for the best-fit Z_{metal} = 0.008 sed@ models for a grid of ages and extinctions. The contour levels are arbitrarily chosen to be 1, 3 and 10% of the reduced χ^2 minimum, to outline the trends. The left panel shows the contours derived for a continuum-normalised set of deep absorption lines alone (cf. text), the center panel shows the constraints derived from the photometric colours alone, and the right panel shows the combined contours of the two independent sets taken together. The optimal parameter set is age=20±5 Ma, A_V=0.55±0.02

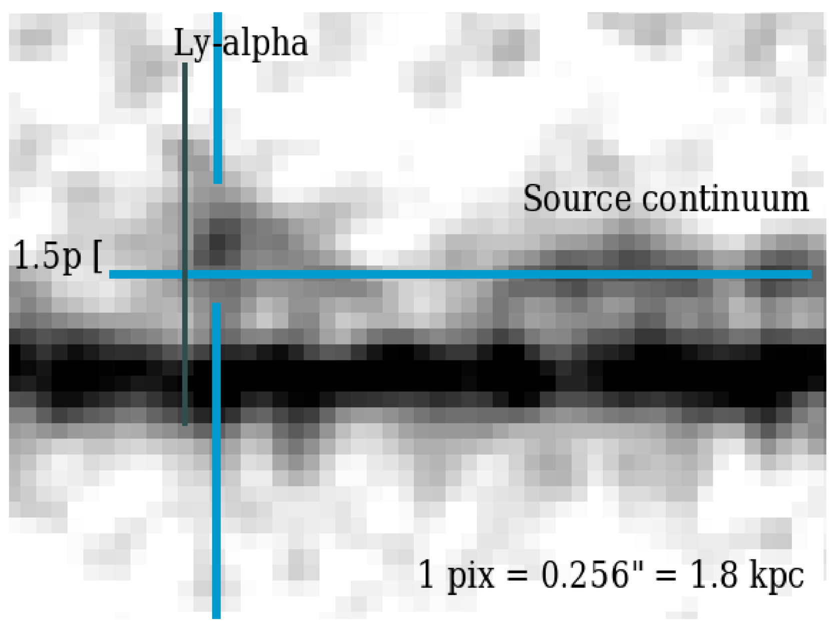

Zoom on the 2-D spectrum around Lyα, showing the spatial offset of ~ 2±0.5 pixels (0.51±0.13 arcsec) and the velocity shift of Δv = +830 km s^{-1}, indicative of outflows (121.567 nm position is the narrow green vertical line). The lower trace is the spectrum of the elliptical galaxy that produces the gravitational lensing effect.

REFERENCES

Ando M., Ohta K., Iwata I., Watanabe C., Tamura N., Akiyama M., Aoki K., 2004, ApJ, 610, 635
Asplund M., Grevesse N., Sauval A. J., 2005, in Barnes T. G., Bash F. N., eds, ASP Conf. Ser. 336: Cosmic Abundances as Records of Stellar Evolution and Nucleosynthesis p. 25
Bentz M. C., Osmer P. S., Weinberg D. H., 2004, ApJl, 600, L19
Berger E., Penprase B. E., Cenko S. B., Kulkarni S. R., Fox D. B., Steidel C. C., Reddy N. A., 2006, ApJ, 642, 979
Bolton A. S., Burles S., Koopmans L. V. E., Treu T., Moustakas L. A., 2006, ApJ, 638, 703
Bolzonella M., Miralles J.-M., Pelló R., 2000, A&A, 363, 476
Buzzoni A., 1989, ApJS, 71, 817
Cabanac R. A., Alard C., Dantel-Fort M., Fort B., Gavazzi R., Gomez P., Kneib J. P., Le Fèvre O., Mellier Y., Pello R., Soucail G., Sygnet J. F., Valls-Gabaud D., 2007, A&A, 461, 813
Cabanac R. A., Valls-Gabaud D., Jaunsen A. O., Lidman C., Jerjen H., 2005, A&A, 436, L21
Castelli F., Kurucz R. L., 1994, A&A, 281, 817
Cerviño M., Luridiana V., 2004, A&A, 413, 145
Cerviño M., Luridiana V., Pérez E., Vílchez J. M., Valls-Gabaud D., 2003, A&A, 407, 177
Cerviño M., Mas-Hesse J. M., 1994, A&A, 284, 749
Cerviño M., Valls-Gabaud D., 2003, MNRAS, 338, 481
Cerviño M., Valls-Gabaud D., Luridiana V., Mas-Hesse J. M., 2002, A&A, 381, 51
Dow-Hygelund C. C., Holden B. P., Bouwens R. J., van der Wel A., Illingworth G. D., Zirm A., Franx M., Rosati P., Ford H., van Dokkum P. G., Stanford S. A., Eisenhardt P., Fazio G. G., 2005, ApJL, 630, L137
Fynbo J. P. U., Starling R. L. C., Ledoux C., et al. 2006, ArXiv astro-ph/0602444
Leitherer C., Schaerer D., Goldader J. D., Delgado R. M. G., Robert C., Kune D. F., de Mello D. F., Devost D., Heckman T. M., 1999, ApJS, 123, 3
Miller G. E., Scalo J. M., 1979, ApJS, 41, 513
Noll S., Mehlert D., Appenzeller I., Bender R., Böhm A., Gabasch A., Heidt J., Hopp U., Jäger K., Seitz S., Stahl O., Tapken C., Ziegler B. L., 2004, A&A, 418, 885
Peng C. Y., Ho L. C., Impey C. D., Rix H., 2002, AJ, 124, 266
Pettini M., Rix S. A., Steidel C. C., Adelberger K. L., Hunt M. P., Shapley A. E., 2002, ApJ, 569, 742
Pettini M., Steidel C. C., Adelberger K. L., Dickinson M., Giavalisco M., 2000, ApJ, 528, 96
Savaglio S., Panagia N., Padovani P., 2002, ApJ, 567, 702
Schaerer D., 2003, A&A, 397, 527
Schaerer D., Pelló R., 2005, MNRAS, 362, 1054
Schaerer D., Vacca W. D., 1998, ApJ, 497, 618
Schaerer D., Verhamme A., 2008, ArXiv e-prints, 801
Shapley A. E., Steidel C. C., Adelberger K. L., Dickinson M., Giavalisco M., Pettini M., 2001, ApJ, 562, 95
Shapley A. E., Steidel C. C., Pettini M., Adelberger K. L., 2003, ApJ, 588, 65
Spitzer L., 1978, Physical processes in the interstellar medium. (New York : Wiley-Interscience)
Steidel C. C., Adelberger K. L., Giavalisco M., Dickinson M., Pettini M., 1999, ApJ, 519, 1
Steidel C. C., Pettini M., Adelberger K. L., 2001, ApJ, 546, 665
Valls-Gabaud D., 1993, ApJ, 419, 7
Valls-Gabaud D., Cabanac R., Lidman C., Diego J. M., Saha P., 2006, in Mamon G. A., Combes F., Deffayet C., Fort B., eds, EAS Publications Series Vol. 20 of EAS Publications Series. pp 149–152
Vázquez G. A., Leitherer C., 2005, ApJ, 621, 695
Verhamme A., Schaerer D., Maselli A., 2006, A&A, 460, 397
Vreeswijk P. M., Ellison S. L., Ledoux C., et al. 2004, A&A, 419, 927
Vreeswijk P. M., Smette A., Fruchter A. S., et al. 2006, A&A, 447, 145